ANALYSIS OF VEGETATION INDEX NDVI ANISOTROPY TO IMPROVE THE ACCURACY OF THE GOES-R GREEN VEGETATION FRACTION PRODUCT

Yuhong Tian[1], Peter Romanov[2], Yunyue Yu[3], Hui Xu[1], Dan Tarpley[4]

1. I.M. Systems Group at NOAA-NESDIS-STAR, 5200 Auth Rd, Camp Springs, MD 20746, USA
2. CICS, University of Maryland, College Park, MD 20742, USA
3. NOAA-NESDIS-STAR, 5200 Auth Rd, Camp Springs, MD 20746, USA
4. Short and Associates, 5200 Auth Rd, Camp Springs, MD 20746, USA

ABSTRACT

Green Vegetation Fraction (GVF) is the fraction of area within the instrument footprint occupied by green vegetation. Information on GVF is needed to estimate the surface energy balance in numerical weather prediction (NWP) and climate models. For the Geostationary Operational Environmental Satellite-R Series (GOES-R) Advanced Baseline Imager (ABI) algorithm development, a normalized difference vegetation index (NDVI) based linear mixture algorithm has been chosen to convert NDVI into GVF. The GVF algorithm has been developed and tested using a proxy dataset from the Spinning Enhanced Visible and Infrared Imager (SEVIRI) sensor onboard the European Meteosat Second Generation (MSG) geostationary satellite. Studies of SEVIRI data have shown that NDVI strongly depends upon the viewing and illumination geometry of observations, especially over dense vegetation. If not corrected, this angular anisotropy of NDVI causes substantial spurious diurnal variations in the derived GVF. An empirical kernel-driven model to correct NDVI for angular anisotropy has been developed and implemented in the GVF algorithm. Its kernel weights for the GVF algorithm were also determined empirically from the SEVIRI clear-sky data. The preliminary validation estimates show that the model's performance is good.

Index Terms— Remote Sensing, geostationary satellite, NDVI, angular anisotropy, modeling

1. INTRODUCTION

The green vegetation fraction (GVF) is defined as the fraction of the area within the instrument footprint occupied by green vegetation. The Numerical Weather Prediction (NWP) and climate models need this parameter to partition the fraction of the surface in the model grid cell that is evaporating and transpiring at rates controlled by vegetation as opposed to the fraction of the surface that is evaporating overbare soil surface. The most common approach to estimating the GVF involves the use of the normalized difference vegetation index (NDVI) and a linear mixture model with two endmembers representing fully vegetated land surface and bare ground [1-2]:

$$GVF = \frac{NDVI - NDVI_{min}}{NDVI_{max} - MDVI_{min}}$$

In the formula NDVI is the observed value, $NDVI_{max}$ is the maximum NDVI corresponding to 100% vegetation cover, and $NDVI_{min}$ is the minimum NDVI corresponding to 0% vegetation cover or bare soil. All the three terms NDVI, $NDVI_{max}$ and $NDVI_{min}$ are top of the atmosphere (TOA) values. This approach to estimating the GVF was adopted to generate the GVF product from the Geostationary Operational Environmental Satellite-R Series (GOES-R) Advanced Baseline Imager (ABI).

The development of the GVF algorithm faces one principal challenge. The NDVI value depends on the observational geometry. This occurs due to different angular anisotropies of reflectance in the visible and near-infrared spectral bands contributing to the NDVI. Many applications implicitly assume that angular effects on NDVI are neglectable. However, it has been demonstrated that TOA NDVI depends on atmospheric path scattering and land surface bidirectional reflective properties [3]. To achieve consistent retrievals of GVF both in space and time a proper mechanism to correct NDVI for angular effects before being used is needed.

In this paper we will fist analyze the characteristics of NDVI angular anisotropy from observed and model simulated data, and then develop an empirical kernel-driven model to correct the NDVI angular effect.

2. DATA

The ABI is being developed as the future imager on the GOES series, slated to be launched in approximately 2015 with GOES-R. Similar to the current GOES imager, the ABI will be used for a wide range of qualitative and quantitative

weather, oceanographic, climate, and environmental applications. It will offer more spectral bands, higher spatial resolution, and faster imaging than the current GOES imager. The ABI spatial resolution will be nominally 2 km for the infrared bands and 0.5 km for the 0.64-μm visible band. The instrument will allow a flexible scanning scenario. One of the modes is that the ABI will scan the full disk in every 15 min, plus the continental United States 3 times [4]. The GVF product will be generated over clear sky conditions during daytime for the GOES-R full disk area and will be delivered on an hourly basis.

Observations from the Spinning Enhanced Visible and Infra-red Imager (SEVIRI), onboard the European Meteosat Second Generation (MSG) satellite, are used as proxy for the GOES-R ABI in the GVF algorithm development. Both the MSG and GOES-R are geostationary satellites. The SEVIRI spectral channels in the visible and near infrared spectrum are close to the ABI channels. The MSG SEVIRI has 11 spectral bands centered in the visible and in the infrared portion of the spectrum. The spatial resolution of MSG SEVIRI observations is 3 km, and the observations are made at an 15 minutes interval. The close similarity between SEVIRI and ABI makes it reasonable for us to use the SEVIRI observations to develop and test the GVF algorithm.

MSG 30-min images for the time period from Feb 2007 to Feb 2008 have been used. A special interactive system was built to help visualize and analyze daily time series of MSG reflectances and NDVI. Data for two days of every month have been examined. Cloud clear daily time series were selected interactively. Images were examined visually. Time series of reflectance and temperature were checked for smoothness. Overall about 880 daily time series of reflectance and NDVI were identified and saved. These data are located in Europe, Asia and Africa within the SEVIRI domain.

3. DATA ANALYSIS RESULTS

Examination of diurnal time series of clear sky NDVI has revealed a strong angular anisotropy inherent to NDVI values (Figure 1). It is found that the change of solar zenith angle may cause up to a change of 0.4 in the NDVI value. The effect of the solar-satellite relative azimuth on NDVI is smaller, but may still cause a change of about 0.1 in NDVI. The NDVI dependence on relative azimuth may result in an asymmetry in the NDVI daily change. Overall the angular anisotropy in NDVI increases with the NDVI values.

In order to understand how atmospheric effects influence the NDVI anisotropy seen by satellites, the "second simulation of a satellite signal in the solar spectrum" (6S) code and Boston University's BRDF model

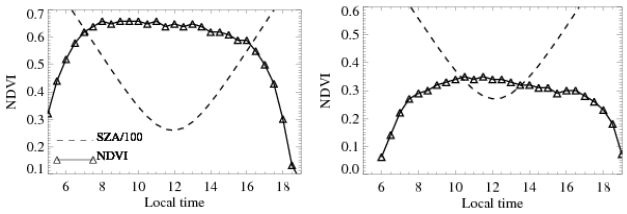

Fig. 1: Examples of NDVI daily change (as function of solar zenith angle/local time) from July 2007 MSG-SEVIRI cloud-clear data. The vegetation types are mixed forest (Right) and cropland (Left).

were used to simulate the top of canopy (TOC) and TOA reflectance and NDVI with aerosol optical depth (AOD) of 0.05, 0.15, 0.25 and 0.45, respectively. Three different vegetation types (dense broadleaf tree-shrubs, dense needle leaf trees-shrubs, and dense grass like vegetation - crops) and three different soil types (smooth dark soil, smooth bright soil, rough bright) were used in this work.

Figure 2 shows that the magnitude of NDVI generally decreases with the increase of AOD. Bidirectional NDVI at TOA features with an overall dome shape when canopy was measured from the near-nadir view to larger view angles. As the viewing or solar zenith angle increases, the atmospheric contribution to TOA reflectance increases and thus causes a TOA bidirectional NDVI decrease. In addition, the change from a bowl shape of NDVI at TOC to mostly a dome shape at TOA indicates that the decrease of NDVI resulting from atmospheric scattering is larger than the increase of surface NDVI as the viewing zenith angle increases.

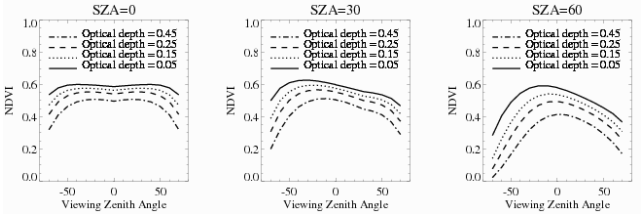

Fig. 2: Simulated TOA NDVI as function of view zenith angle, with the aerosol optical depth of 0.05, 0.15, 0.25, and 0.45, respectively. The vegetation type used in this simulation is dense needleleaf trees-shrubs.

The above results indicate that although geostationary satellites making repeat observation over a given region can provide high temporal resolution data, changes in satellite viewing zenith angles over different locations on Earth may bring large uncertainties to GVF, e.g., the NDVI measured from larger viewing zenith angles will be underestimated even at the overhead sun condition. In addition, for a given location, the change in the observational geometry with local time also causes substantial spurious diurnal variations in the derived GVF. GVF is used to characterize vegetation cover properties and thus should not depend on the

observational geometry. Therefore, to provide consistent estimates of GVF all TOA NDVI measurements should be brought to a reference geometry before being used to estimate GVF.

4. NDVI ANGULAR ANISOTROPY MODEL

4.1. Model development

Kernel-driven models have been widely used to reproduce anisotropy of the land surface reflectance and to calculate albedo [5-6]. In this study we have developed a similar approach to measured NDVI and proposed the following simple analytical model relating the NDVI to the observation geometry,

$$NDVI(\theta_s, \theta_v, \varphi) = NDVI(0,0,0)[1 + C_1 f_1 + C_2 f_2]$$

Where f_1 and f_2 are kernel functions, C_1 and C_2 are kernel weights, φ is relative azimuth, Θ_S is solar zenith angle and Θ_V is satellite zenith angle.

In this equation, the first kernel function is meant to characterize the NDVI change with solar and satellite zenith angle $f_1 = (tan\theta_s + tan\theta_v)$, and the second kernel function capture the NDVI azimuth change $f_2 = (cos\varphi + 1)^2 (tan\theta_s\, tan\theta_v)^{1/2}$.

The NDVI anisotropy model assumes reciprocity of viewing and illumination angles. Two kernel weights C_1 and C_2 were determined from the SEVIRI clear sky observations using the following empirical approach.

For two observations taken over the same scene during one day at different illumination conditions *NDVI (0,0,0)* should be the same, hence we have:

$$\frac{NDVI(\theta_{s1}, \theta_{v1}, \varphi_1)}{1 + C_1 f_{11} + C_2 f_{21}} = \frac{NDVI(\theta_{s2}, \theta_{v2}, \varphi_2)}{1 + C_1 f_{12} + C_2 f_{22}}$$

Where $f_{11} = (tan\theta_{s1} + tan\theta_{v1})$, $f_{12} = (tan\theta_{s2} + tan\theta_{v2})$, $f_{21} = (cos\varphi_1 + 1)^2 (tan\theta_{s1}\, tan\theta_{v1})^{1/2}$ and $f_{22} = (cos\varphi_2 + 1)^2 (tan\theta_{s2}\, tan\theta_{v2})^{1/2}$. The observational geometry $(\theta_{s1}, \theta_{v1}, \varphi_1)$ is for the first measurement, and $(\theta_{s2}, \theta_{v2}, \varphi_2)$ is for the second measurement. Since the target is the same, the satellite zenith angle does not change: $\theta_{v1} = \theta_{v2}$.

Reformulating the above equation we have:

$$\begin{aligned} NDVI(\theta_{s1}, \theta_{v1}, \varphi_1) - NDVI(\theta_{s2}, \theta_{v2}, \varphi_2) \\ = C_1[NDVI(\theta_{s2}, \theta_{v2}, \varphi_2) f_{11} \\ - NDVI(\theta_{s1}, \theta_{v1}, \varphi_1) f_{12}] \\ + C_2[NDVI(\theta_{s2}, \theta_{v2}, \varphi_2) f_{21} \\ - NDVI(\theta_{s1}, \theta_{v1}, \varphi_1) f_{22}] \end{aligned}$$

Hence we obtain a system of linear equations to determine coefficients C_1 and C_2 based on a set of pairs of observations taken over the same scene but under different illumination conditions. In this equation, all are known except C_1 and C_2, which can be derived by using a multiple linear regression based on a set of pairs of observations taken over the same scene but under different illumination conditions.

The SEVIRI data is used as the ABI proxy data for our algorithm development to determine C_1 and C_2. First, about 5% of the 880 clear sky NDVI daily time series mentioned in section 2 were used. The algorithm was then tested over all the 800+ records in the archive. The best fit is: C_1 = -0.0723 and C_2 = -0.0101. Note that C_1 and C_2 are global values for every pixel.

4.2. Model testing

The performance of the NDVI angular model is tested using the SRVIRI data. Criteria characterizing the validity of NDVI anisotropy model include its capability to (1) accurately reproduce the observed NDVI diurnal change; and (2) to correct the decrease of scatter in the diurnal time series of the NDVI (or bring the NDVI to a common sun-satellite geometry) as compared to the original observed NDVI. The evaluation of the NDVI angular anisotropy model is based on these two criteria.

4.2.1 NDVI observed versus NDVI predicted

The hourly NDVI can be predicted using only one value of NDVI observed close to local noon time:

$$\begin{aligned} NDVI(\theta_{s2}, \theta_{v2}, \varphi_2) \\ = \frac{NDVI(\theta_{s1}, \theta_{v1}, \varphi_1)}{1 + C_1 f_{11} + C_2 f_{21}} (1 + C_1 f_{12} \\ + C_2 f_{22}) \end{aligned}$$

Here $NDVI(\theta_{s1}, \theta_{v1}, \varphi_1)$ is the NDVI observed at the local noon, and $NDVI(\theta_{s2}, \theta_{v2}, \varphi_2)$ is the predicted NDVI at anytime under cloud clear conditions within the same day. Since the target is the same, $\theta_{v1} = \theta_{v2}$. Figure 3 shows that the NDVI model can reproduce well the observed NDVI diurnal changes.

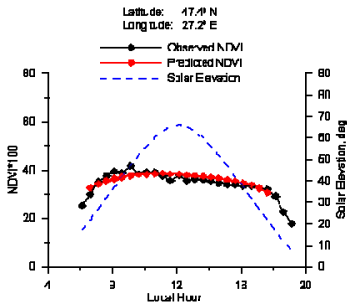

Fig. 3: Comparison of NDVI daily change between the original observed SEVIRI and the predicted using the angular anisotropy model.

The diurnal time series of NDVI over the 880 locations in Europe, Asia and Africa within the SEVIRI domain (as described in section 2) have been used to test the accuracy of the model. For each NDVI diurnal time series, we have calculated the value of the root mean square error (RMSE). The mean RMSE over all of the 880 cases is 0.032.

4.2.2 NDVI observed versus NDVI corrected to a reference geometry

Given every individual $NDVI(\theta_{s1}, \theta_{v1}, \varphi_1)$ observation within a day, corresponding NDVI that is brought (corrected) to the reference sun-satellite geometry, $NDVI(\theta_{s2} = 45°, \theta_{v2} = 45°, \varphi_2 = 90°)$, can be calculated using the same formula as in section 4.2.1.

The performance of the NDVI angular correction is evaluated by comparing the root mean square difference (RMSD) of NDVI in the diurnal time scale. The RMSD is calculated as,

$$RMSD = \sqrt[2]{\frac{\sum_{i=1}^{n}(NDVI_i - \overline{NDVI})^2}{n}}$$

Where $NDVI_i$ is either the NDVI corrected to the reference geometry or the original measured one in a diurnal time scale for one pixel, n is the total number of clear sky measurements in a whole day for that pixel, and ??? is the corresponding mean NDVI (calculated from angularly corrected NDVI or original measured NDVI) in that day. The detail procedure is as follows. First, hourly clear-sky NDVI (angularly corrected and originally measured) for every location are collected. Second the diurnal NDVIs RMSD is calculated. Last, the frequency distribution of RMSD for all pixels is showed in Figure 4.

The values in blue in Figure 4 show the results from the original observed NDVI daily record. Those in red are the results from the corrected NDVI. Lower RMSD values means less diurnal changes. After the angular correction, there are significantly more cases of small RMSD, indicting

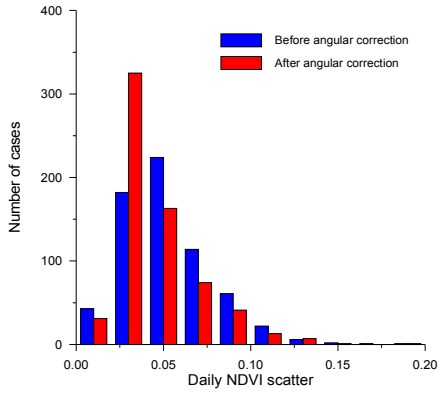

Fig. 4: Statistics of RMSD in daily NDVI records before and after the angular correction applied to the 880 daily time series of SEVIRI NDVI as mentioned in section 3.4.2. The x axis is NDVI RMSD value.

that the NDVI brought to the reference sun-viewing geometry has less scatter at daily time scale as compared to the original NDVI. However, the anisotropical correction reduces the scatter in the NDVI daily time series but does not eliminate the diurnal change completely.

4. REFERENCES

[1] G. Gutman and A. Ignatov, "The derivation of the green vegetation fraction from NOAA/AVHRR data for use in numerical weather prediction models", *Int. J. Remote Sens.*, 19 (8), 1533–1543, 1998.

[2] L. Jiang, F. N. Kogan, W. Guo, J. D. Tarpley, K. E. Mitchell, M. B. Ek, Y. Tian, W. Zheng, C.-Z. Zou, and B. H.Ramsay, "Real-time weekly global green vegetation fraction derived from advanced very high resolution radiometer-based NOAA operational global vegetation index (GVI) system,", *J. Geophys. Res.*, 115, D11114, doi:10.1029/2009JD013204, 2010.

[3] F. Gao, Y. Jin, X. Li, C. Schaaf, and A. H. Strahler, Bidirectional NDVI and Atmospherically Resistant BRDF Inversion for Vegetation Canopy, *IEEE Trans. Geosci. Remote Sens.*, 40, 1269-1278, 2002.

[4] T. J., Schmit, M. M. Gunshor, W. P. Menzel, J. J. Gurka, J. Li, and A. S. Bachmeier, "Introducing the next-generation Advanced Baseline Imager on GOES-R," *BAMS*, pp. 1079-1096, 2005

[5] J.-L. Roujean, M. Leroy, and P. Y. Deschamps "A bidirectional reflectance model of the Earth's surface for the correction of remote sensing data," *J. Geophys. Res.*, vol. 97, pp. 20 455–20 468, 1992.

[6] Lucht, W., C.B. Schaaf, and A.H. Strahler, "An Algorithm for the retrieval of albedo from space using semiempirical BRDF models," *IEEE Trans. Geosci. Remote Sens.*, 38, 977-998, 2000.